International Journal of Material Forming (2023) 16:7
https://doi.org/10.1007/s12289-022-01729-w

REVIEW

Residual stresses and deformations of laser additive manufactured metal parts: a review

Bo He[1] · Cheng Bi[1] · Xiaodan Li[2] · Wei Wang[1] · Guang Yang[1]

Received: 13 July 2022 / Accepted: 28 November 2022 / Published online: 12 December 2022
© The Author(s), under exclusive licence to Springer-Verlag France SAS, part of Springer Nature 2022

Abstract

Laser additive manufacturing (LAM) technology is based on three-dimensional digital models, using laser as an energy source to melt metal materials layer by layer to form target parts. LAM technology can produce metal parts with complex structures, but the residual stress generated during the LAM process causes deformation. Therefore, in order to facilitate wide application of LAM parts in industry, it is of great significance to improve the dimensional accuracy and reduce the deformation of the LAM parts. This paper summarizes the factors affecting the residual stress and deformation of LAM parts, introduces the methods commonly used to detect the residual stress and deformation of LAM parts, and compares their applications, advantages and disadvantages, expounds five methods for predicting the deformation of LAM parts, introduces the deformation compensation method based on the reverse compensation principle, and puts forward the deformation detection method that may be employed to LAM parts in the future.

Keywords Laser additive manufacturing · Residual stress detection · Deformation detection · Deformation prediction · Deformation compensation

Introduction

Laser Additive Manufacturing (LAM) technology, which is based on three-dimensional digital models, melts metal materials (powder or wire) by laser and forms target metal parts layer by layer [1]. LAM technology has the characteristics of direct forming in three-dimensional space and can be used to form complex structures which cannot be manufactured by traditional processes, greatly reducing or even eliminating structures reserved for process and structures for assembly. In addition, fabrication of new types of alloy parts can be achieved by changing the composition of the metal powder or wire [2–4]. The fusion of metal wire in LAM is called Laser and Wire Additive Manufacturing (LWAM) technology, and the fusion of metal powder mainly includes Selective Laser Melting (SLM), Laser Deposition Manufacturing (LDM) and Direct Metal Laser Sintering (DMLS). SLM, also called Laser Powder Bed Fusion (L-PBF), uses laser as heat source to scan the metal powder bed layer by layer according to the path planned in the CAD slice model. The scanned metal powders are molten and solidified, and finally the required metal parts can be obtained [5]. LDM, also called Laser Directed Energy Deposition (LDED), uses high-energy laser beam as heat source to melt and deposit synchronously fed metal powders layer by layer to realize the manufacture of metal parts [6]. DMLS uses high-energy laser beam to fuse the powders at specified locations in each layer of the powder bed, binds the metal particles together through liquid phase sintering, and scans layer by layer until the part is fabricated [1].

In LAM, laser beam melts metal material to form a molten pool. After the laser beam scanning is completed, the molten pool rapidly solidifies and fuses with the previous

✉ Bo He
hebo1978@163.com

Cheng Bi
1661649672@qq.com

Xiaodan Li
lixd014@avic.com

Wei Wang
wwei24@qq.com

Guang Yang
yangguang@sau.edu.cn

[1] School of Mechatronics Engineering, Shenyang Aerospace University, Shenyang 110136, China

[2] AVIC Shenyang Aircraft Company Limited, Shenyang 110850, China

layer, and the material in the molten pool shrinks when it is cooled. As the number of layers increases, the material near the molten pool is subjected to repeated thermal cycling, resulting in alternate expansion and contraction [7–11]. Thermal gradients and thermal cycles in the layer-by-layer manufacturing process lead to the accumulation of internal stress. If the internal stress does not exceed the yield strength of the part, residual stress will be generated inside the formed part. Otherwise, the part will deform or crack. Deformation will reduce the dimensional accuracy of the part, and cracking will destroy the integrity of the part and reduce the macro-mechanical properties of the part [12, 13]. At present, some researchers have summarized and discussed the residual stress or deformation in the SLM process [14, 15]. Besides SLM, discussions of residual stress and deformation in other metal LAM processes, such as LDM and DMLS, are included in this article.

Factors affecting residual stress and deformation of LAM metal parts

Repeated heating and cooling in the LAM process causes temperature gradients in the parts, generating residual stress. Formed parts may deform or even crack, and severe deformation or crack may render the part unusable. In order to control the residual stress and deformation of parts fundamentally, it is necessary to study the factors that affect the deformation of parts manufactured by LAM. Process parameters are one group of the important factors affecting the residual stress and deformation of LAM, including laser power, scanning speed, powder layer thickness, hatch spacing and preheating temperature, etc. Ali et al. [16] studied the effect of different combinations of laser power and exposure on residual stress while keeping the energy density unchanged. It was found that the combination of low laser power and high exposure reduced the temperature gradient and cooling rate, resulting in the decrease of residual stress in SLM fabricated Ti6Al4V parts. At the same time, the effect of powder layer thickness on residual stress was explored, and it was concluded that the temperature gradient decreased with the increase of layer thickness, so increasing the layer thickness would lead to a decrease of residual stress. Mugwagwa et al. [17] studied the effect of process parameters on the deformation of SLM parts, and found that the increase of the scanning speed would increase the temperature gradient and cooling rate, resulting in the increase of the deformation of the cantilever beam part. At the same time, it was found that the deformation increased with the decrease of the porosity of the cantilever beam part. The porosity of the part was greater at a layer thickness of 45 μm compared to a layer thickness of 30 μm, so increasing the layer thickness could reduce the deformation of the SLM cantilever beam part. Jiang et al. [18] studied the effects of substrate preheating and scanning speed on the residual stress of SLM fabricated AlSi10Mg parts, and found that when the substrate was preheated to a certain temperature, the temperature gradient between the substrate and the molten pool was reduced, which reduced the residual stress in the part. Increasing the laser scanning speed could increase the cooling rate of the molten pool and reduce the temperature gradient of the part, thereby reducing the residual stress of the part. Malý et al. [19] studied the effect of process parameters on residual stress and deformation of Ti6Al4V parts formed by SLM, and found that the increase of preheat temperature or laser power would reduce the deformation of SLM parts, and increasing the laser scanning speed and real delay would increase the deformation of SLM parts. Because the reduced scanning speed, increased preheat temperature, and reduced waiting time could reduce cooling rate, thereby reducing the temperature gradient, residual stress and deformation of the part. Levkulich et al. [20] studied the factors that affected the residual stress and deformation of SLM formed Ti6Al4V parts. The results show that the residual stress on the top surface of the part decreases with the increase of the deposition height, and the residual stress on the bottom surface of the substrate increases with the increase of the deposition height. Lowering the scanning speed and increasing the laser power can reduce residual stress on the top surface of the part and the bottom surface of the substrate.

There are some seemingly contradictory conclusions in the above literatures about the effects of laser power and scanning speed on the residual stress and deformation of parts. Xiao et al. [21] studied the stress evolution process during the SLM process of Ti6Al4V parts. The residual stresses under different scanning speeds and laser powers were measured when the hatch spacing was 0.1 mm (Fig. 1a), and the residual stresses under different hatch spaces and laser powers were measured as well when the scanning speed was 1000 mm/s (Fig. 1b). The results show that with the increase of laser power, scanning speed and hatch spacing, the variation of residual stress is different, and it is not a monotonous increase or decrease.

In addition to the above factors, another important factor that affects the residual stress and deformation of LAM parts is the laser scanning strategy. Similar to the process parameters, it is believed that the scanning strategy affects the residual stress and deformation of the part by affecting the heat input distribution. Commonly used scanning strategies include unidirectional line scanning, reciprocating line scanning, helical line scanning, island scanning and interlayer rotation scanning strategies (take 90° rotation as example), as shown in Fig. 2.

Cheng et al. [22] studied the residual stress and deformation of SLM manufactured Inconel 718 parts under the

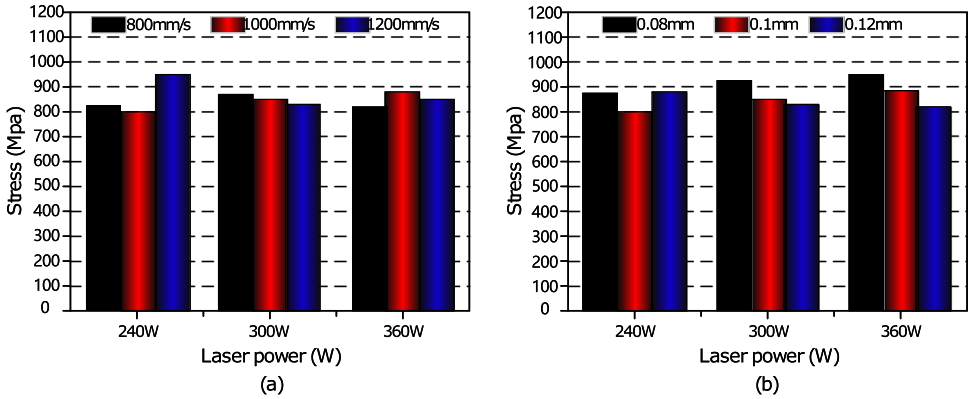

Fig. 1 Relationship between residual stress and process parameters (**a**) hatch spacing was 0.1 mm; (**b**) scanning speed was 1000 mm/s [21]

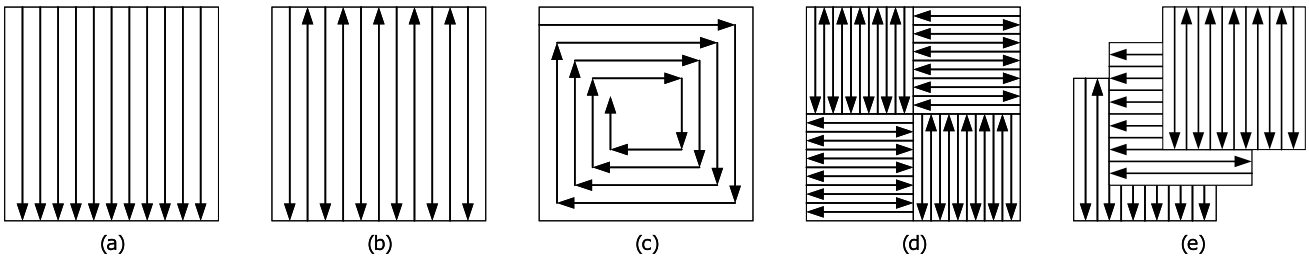

Fig. 2 Common scanning strategies (**a**) unidirectional line scanning; (**b**) reciprocating line scanning; (**c**) helical line scanning; (**d**) island scanning; (**e**) interlayer rotation scanning (take 90° rotation as example)

strategies of island scanning, 0° and 45° reciprocating scanning, 45°, 90° and 67° interlayer rotating scanning, and out-in and in–out helical scanning. It was found that the parts manufactured by the in–out helical line scanning strategy had the largest residual stress perpendicular to the deposition direction, and the parts manufactured by the 45° reciprocating line scanning strategy had the smallest residual stress perpendicular to the deposition direction. The parts manufactured by the in–out helical line scanning strategy had the largest deformation in the deposition direction, and the parts manufactured by the 45° reciprocating line scanning strategy have the smallest deformation in the deposition direction. Ali et al. [23] studied the influences of 45° and 90° interlayer rotation scanning, 2 mm × 2 mm, 3 mm × 3 mm and 5 mm × 5 mm island scanning, and 5 mm × 5 mm island scanning strategy of 45° and 90° adjacent partition rotation on the residual stress of Ti6Al4V parts formed by SLM. The residual stress could be reduced by rotating scanning on adjacent sections, and the effect of rotating 90° was more obvious. However, the residual stress of parts manufactured by 90° interlayer rotation scanning strategy was the smallest. Song et al. [24] studied the influences of reciprocating line scanning strategy and 15° and 90° interlayer rotation scanning strategy on the residual stress of Ti6Al4V parts formed by SLM. It was found that the residual stress of parts manufactured with 15° interlayer rotation scanning strategy was the minimum. Wang et al. [25] studied the influence of reciprocating line scanning strategy and three scanning strategies which were independently developed (normal partition strategy (Fig. 3a), oblique line and layer-staggered divisional strategy (Fig. 3b), spiral divisional strategy (Fig. 3c)) on SLM formed 316L parts. The results show that the parts manufactured by the layer-staggered divisional strategy have better performance, and the formed parts obtain 99.37% density, which effectively improves the distribution of residual stress and alleviates the deformation of the parts.

For the island scanning strategy, the scanning order of all sub-sectors also affects the residual stress and deformation of the part besides the factors of the length and direction of the scanning vector. Mugwagwa et al. [26] studied the effects of island (sub-sectors were scanned randomly),successive (sub-sectors were scanned one after the other), successive chessboard (sub-sectors with horizontal scan vectors were scanned sequentially before the scanning of vertical-vector partitions) and least heat influence (the next partition to scan was as far away as possible from the current sub-sectors) scanning strategies on residual stress and deformation of SLM parts, the scanning sequence was shown in Fig. 4. The vector directions between adjacent islands were shown in Fig. 5. The results show that the continuous scanning strategy obtains the smallest average residual stress and the smallest deformation as well. Mugwagwa et al. [26] concluded that the higher heat accumulation of the successive chessboard

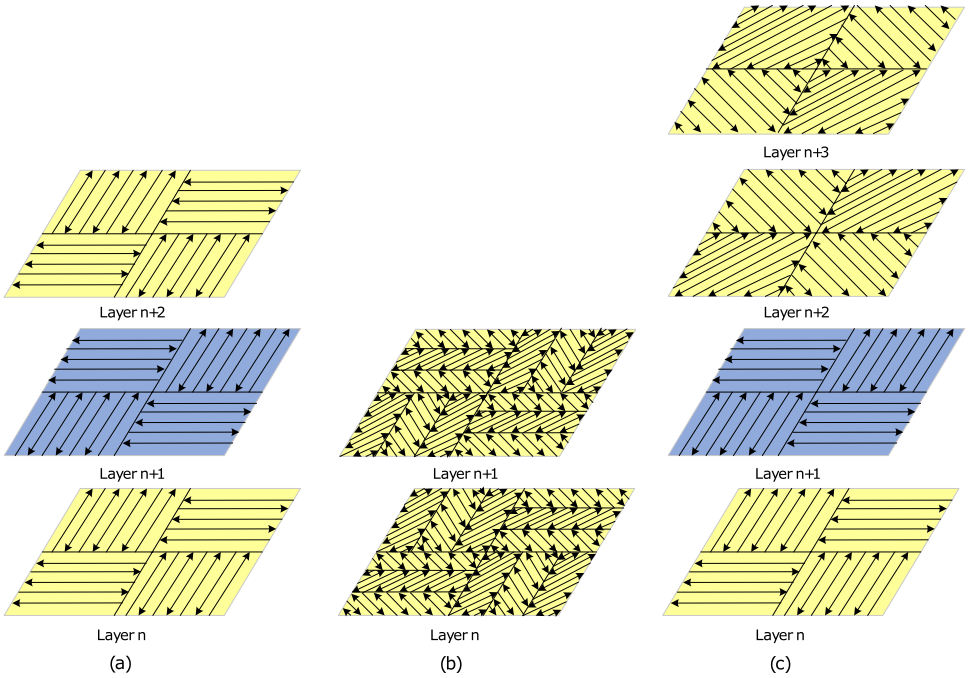

Fig. 3 Self-developed scanning strategy (**a**) normal partition strategy; (**b**) oblique line and layer-staggered divisional strategy; (**c**) spiral divisional strategy [25]

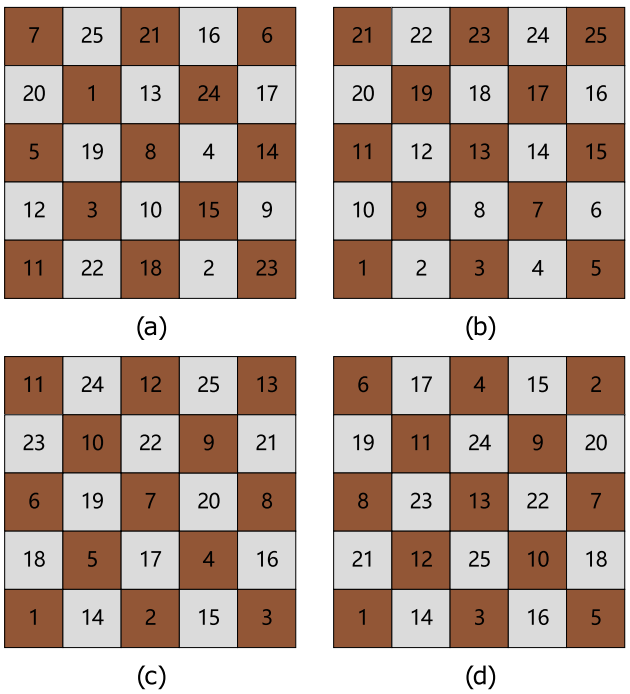

Fig. 4 Scanning strategies for different scan orders (**a**) island(approximation); (**b**) successive; (**c**) successive chessboard; (**d**) least heat influence [26]

scanning strategy compared to the least heat influence and island scanning strategy helped to reduce the temperature difference between adjacent sub-sectors, thereby reducing the resulting stress.

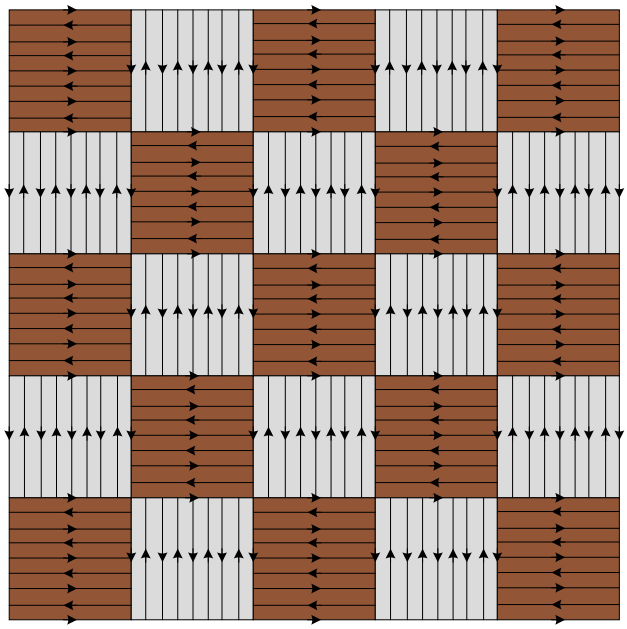

Fig. 5 Scan vector direction between adjacent partitions [26]

Residual stress detection of LAM metal parts

Accurately obtaining the residual stress and deformation data of parts is the key to objectively studying the residual stress and related deformation of LAM parts. The detecting methods for residual stress of LAM parts are divided into destructive methods and non-destructive methods.

Destructive methods include hole-drilling method and contour method, etc., and non-destructive methods include X-ray diffraction method and neutron diffraction method, etc. These residual stress measuring methods are listed in Table 1.

Hole-drilling method

The measurement principle of hole-drilling method is shown in Fig. 6. A small hole with a diameter of 2a is drilled at the position to be measured. The residual stress around the small hole is released, and the material undergoes a slight morphological change. According to the measured strain released, the residual stress at the measured location can be obtained [27]. The calculation formula is as follows.

$$\sigma_{1,2} = \frac{1}{4A}(\varepsilon_1 + \varepsilon_2) \pm \frac{\sqrt{2}}{4B}\sqrt{(\varepsilon_1 - \varepsilon_3)^2 + (\varepsilon_2 - \varepsilon_3)^2} \quad (1)$$

$$\tan\ 2\theta = \frac{\varepsilon_1 + \varepsilon_2 - 2\varepsilon_3}{\varepsilon_1 - \varepsilon_2} \quad (2)$$

In the formula, ε_1, ε_2, and ε_3 are the released strain in three directions. A and B are the release coefficients; θ is the angle between the principal stress σ_1 and strain ε_1; σ_1 and σ_2 are the principal residual stresses. Heigel et al. [28] established a coupled thermal–mechanical model of LDM parts to predict the temperature and stress of Ti6Al4V parts during the LDM process. The hole-drilling method was used to measure the residual stress and laser displacement sensors were used to measure the deflection of parts. The model can predict the stress accurately.

Contour method

According to contour method, the workpiece is cut along the specific target plane (usually by electric spark wire cutting), the residual stress perpendicular to the cutting surface is released without the constraint of the workpiece itself, resulting in the deformation of the cutting surface, and the deformation is proportional to the residual stress perpendicular to the target plane. According to the Bueckner superposition principle, the original stress field of the target plane can be derived by using finite element modeling, and the residual stress of the workpiece perpendicular to the cutting plane can be obtained [29]. The measurement principle is shown in Fig. 7.

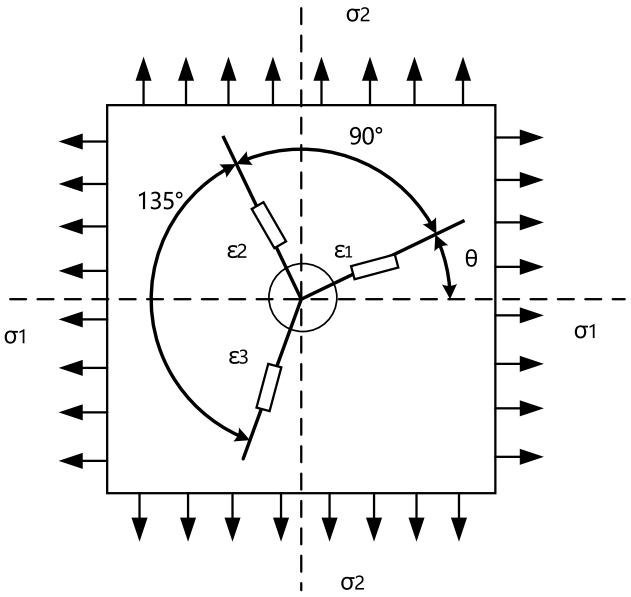

Fig. 6 Schematic diagram of hole-drilling method

Vrancken et al. [30] measured the residual stress of Ti6Al4V manufactured by SLM by the contour method and drew a two-dimensional strain diagram in order to study the influence of residual stress of SLM parts on their mechanical properties. Ahmad et al. [31] measured the residual stress of Ti6Al4V and Inconel 718 parts manufactured by SLM in the deposition direction by the contour method, and verified the numerical model proposed to predict residual stress.

X-ray diffraction method

The measurement principle of X-ray diffraction method (XRD) is shown in Fig. 8. When there is residual stress in the sample, the crystal plane spacing changes. The diffraction peak generated moves accordingly when Bragg diffraction occurs, the moving distance is related to the stress. The residual stress can be obtained by irradiating the sample with X-ray with wavelength λ and measuring the corresponding diffraction angle 2θ [32, 33]. Due to the properties of

Table 1 Comparison of LDM part stress measurement methods

Method	Category	Precision	Application	Features
Hole-drilling method	Semi-destructive testing	High	Surface measurement	Inexpensive equipment, operate easily
Contour method	Destructive testing	High	Large components	Measure stress in vertical cross-sections
X-ray diffraction method	Nondestructive testing	High	Surface measurement	Non-contact
Neutron diffraction method	Nondestructive testing	High	Internal measurement	Penetration is much deeper than X-rays

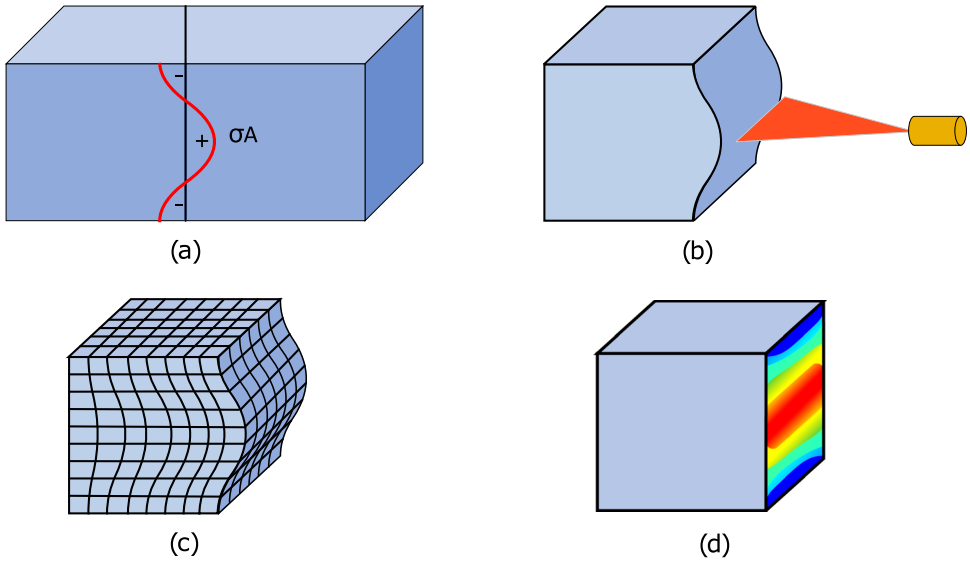

Fig. 7 Basic principle and procedure of residual stress measurement by contour method (**a**) Cutting the part along target plane; (**b**) Measuring the contour of the cutting surface; (**c**) Finite Element Modeling; (**d**) Residual stress distribution

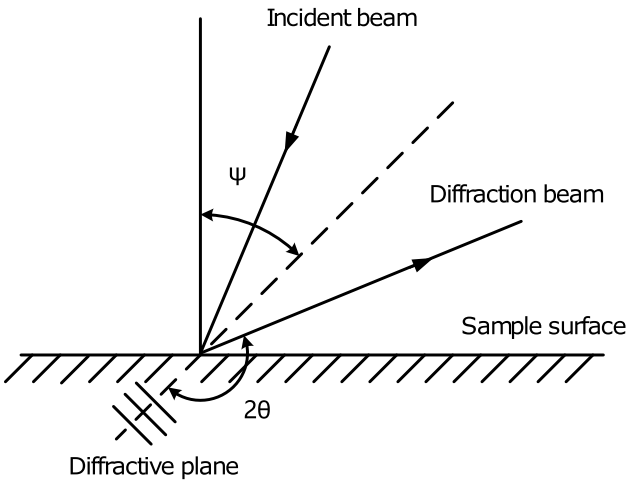

Fig. 8 Schematic diagram of X-ray diffraction method

X-rays, X-ray diffraction method is suitable for measuring residual stresses in fine grained crystalline materials, such as ceramics, metals and intermetallic compounds, and certain composite materials, etc. [34] The depth of penetration of X-rays depends on the anode, material and angle of incidence, and the measured strain is essentially an average of several micrometers of depth below the surface of the specimen. If the material grains are too coarse or the roughness of the surface to be measured is too high, the X-ray diffraction measurement accuracy will be affected greatly [35].

Simson et al. [36] measured the residual stress on the top and the side of 316L parts formed by SLM with X-ray diffraction method, and studied the generation of residual stress and influence of residual stress on SLM parts. The experimental results show that the residual stress of the part is related to the structural density. Kumaran et al. [37] used X-ray diffraction method to measure residual stress of parts and evaluate the residual stresses of 316L parts in SLM and LDM processes.

Neutron diffraction method

Neutron diffraction method employs neutron stream as an incident beam to irradiate the sample, and the diffraction peak is obtained when Bragg diffraction occurs on the crystal surface of the sample. Its measurement principle is similar to that of X-ray diffraction method, but compared with X-ray, neutron has stronger penetration ability and is more conducive to measuring residual stress inside materials or parts [38–40]. Wang et al. [41, 42] proposed a coupled thermo-mechanical model to predict the residual stress of LDM manufactured Inconel 625 thin-wall parts, and used neutron diffraction method to measure the residual stress to verify the model. Subsequently, in-situ neutron diffraction method was used to measure the residual stress of Ti6Al4V parts manufactured by LAM and conventional machining at 600℃ and 700℃, and the stress relaxation behavior and mechanism were studied. Kemerling et al. [43] proposed a finite element model for predicting residual stress of 304L parts manufactured by DMLS. Neutron diffraction method was used to measure the residual stress to verify the model, and the influence of laser scanning strategy on the residual stress of 304L parts formed by DMLS was studied.

Among the commonly used residual stress measurement methods for LAM parts, hole-drilling method has the characteristics of low cost and small measurement depth, so it can only measure the residual stress on the surface of the parts instead of the residual stress inside the parts [27]. Contour method can be used to measure residual stress inside the parts with large thickness. But contour method

can only measure the residual stress perpendicular to the cutting section [27, 29]. At present, X-ray diffraction method is widely used because of its high measurement accuracy and its ability to non-destructively macroscopic macroscopic and microscopic residual stresses. X-ray diffraction is suitable for measuring fine-grained materials. And like the drilling method, X-ray diffraction method can only measure the residual stress on the surface of the material due to its small X-ray penetration depth. If the residual stress inside the part needs to be measured, synchrotron radiation X-ray diffraction method or neutron diffraction method is suitable. Neutrons can penetrate a large depth of the sample and have great advantages in the measurement of the residual stress inside the sample.

Deformation detection of LAM metal parts

The deformation of LAM can be detected by three-coordinate measuring machine, X-ray computer tomography, laser displacement sensor, digital image correlation method and so on.

Coordinate measuring machine

Coordinate measuring machine (CMM) is used to obtain the coordinates of each measuring point on the measured object which is placed in the space of the CMM. According to the spatial coordinate values of these points, the geometric size, shape and position of the measured object are calculated [44]. Dunbar et al. [45] simulated the deformation process with a finite element model and measured the deformation of the formed parts with a three-coordinate measuring machine, in order to verify whether rotational scanning mode and constant scanning mode affect the deformation of SLM parts. It was found that there was little difference between the deformation of the fabricated part with the rotational scanning mode and that of the constant scanning mode. Ning et al. [46] proposed a deformation prediction model of SLM parts, and used this model to predict the deformation of SLM formed Ti6AL4V double cantilever beam parts. At the same time, a three-coordinate measuring machine was used to measure the deformation of the parts, and the prediction results were consistent with the measured results.

X-ray computed tomography

X-ray Computed Tomography (XCT) uses an X-ray tube to emit X-ray beams, the sample to be tested rotates around a fixed axis, the detector collects projection images of the sample at different angles, and then uses a computer to restore the three-dimensional structure of the object model. This measurement method can clearly, accurately and intuitively display the internal structure, composition, material and defect status of the detected object [47, 48]. The principle is shown in Fig. 9.

Samei et al. [49] conducted in-situ uniaxial tensile tests on Cu-4.3Sn alloys fabricated by SLM, and used X-ray computed tomography to visualize the pore growth during part deformation. Choo et al. [50] used high-resolution synchronous X-ray computed microtomography to study the tensile-plastic deformation and fracture behavior of 316L parts fabricated by SLM.

Laser displacement sensor

Laser displacement sensor (LDS) can accurately measure the position and displacement of the target object in a non-contact manner by laser technology [51]. The laser displacement transmitter shoots the laser onto the surface of the object, and a series of reflections present on the surface of the object. One of the reflected rays returns to the laser displacement sensor. According to the angle of light reflection and the distance of laser displacement sensor, the position and displacement of the object can be measured, etc. [52] The measurement principle is shown in Fig. 10.

Denlinger et al. [53] used laser displacement sensors to measure the deformation process of parts in situ, and investigated the effect of interlayer interval on the residual stress and deformation of LDM formed Ti6Al4V and Inconel 625 parts. Corbin et al. [54] used laser displacement sensors to monitor the deformation of parts on site. The effects of substrate thickness, deposition thickness and substrate initial temperature on the deformation of LDM formed Ti6Al4V parts and the effects of substrate thickness and substrate preheating on substrate deformation were investigated.

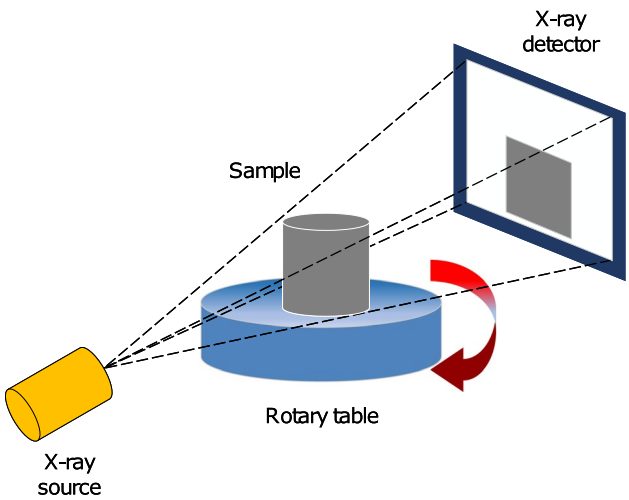

Fig. 9 Schematic diagram of X-ray computed tomography measurement

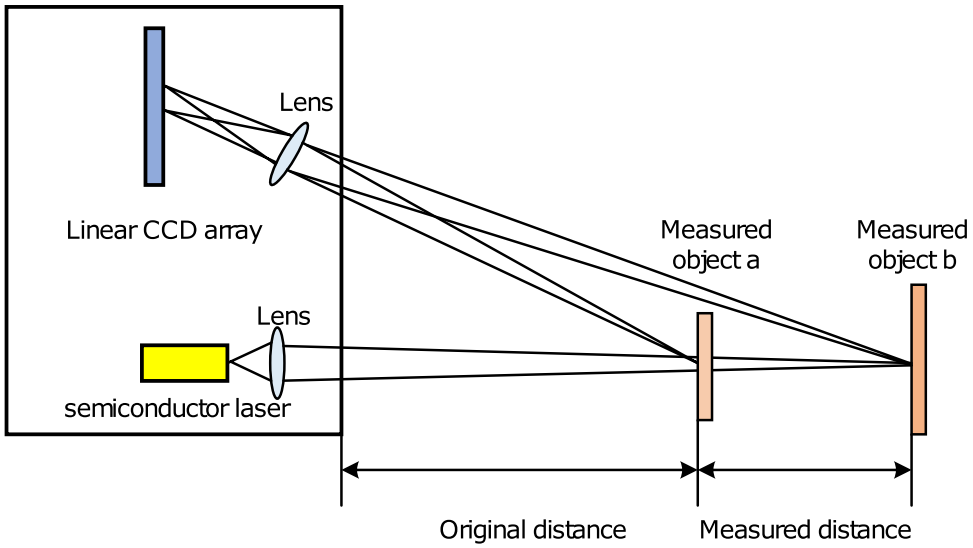

Fig. 10 Schematic diagram of laser displacement sensor measurement

Digital image correlation

Digital Image Correlation (DIC) usually uses a CCD camera to capture images of natural speckle or artificial speckle on the surface of the object before deformation and after deformation, and then the computer detects the displacement by searching for the matching points of the two images [55, 56]. Biegler et al. [57] established a coupled thermal–mechanical model to predict the deformation behavior of LDMed 316L parts. The model was verified by measuring the 3D in-situ deformation of the part online with 3D digital image correlation method. Balit et al. [58] studied the effect of process parameters on the microstructure and properties of LDM manufactured 316L materials. In order to characterize the non-uniform strain and local strain in the microstructure of the parts during the in-situ tensile experiments, in-situ observations were carried out with scanning electron microscopy, combining digital image correlation method and electron backscatter diffraction pattern. Wu et al. [59] studied the effect of microstructure of Ti6Al4V cellular solid with a cuboctahedron structure made by SLM on compressive deformation behavior and fracture mechanism. The deformation and fracture process during the mechanical test were observed by digital image correlation method.

Coordinate measuring machine has high measurement accuracy and can obtain the coordinate values of any point of the measured part [44]. However, due to the limitation of its measurement principle, the full-field deformation data of the part cannot be obtained quickly. Computed tomography technology can visually exhibit the deformation of parts in the form of images [47, 48]. Laser displacement sensor has high measurement accuracy, but its application environment is relatively strict. Digital image correlation is a new type of non-contact optical measurement method, which has the advantages of non-contact, full-field measurement, simple data acquisition process, high measurement accuracy, and low measurement environment requirements. Digital image correlation can measure and characterize the full-field deformation of parts, so it has become more and more widely used in related research in recent years.

Residual stress and deformation prediction of LAM metal parts

The deformation of LAM parts adversely affects the dimensional accuracy and forming quality of the parts, and in severe cases it affects the use of the parts. Therefore, predicting the residual stress and deformation of LAM parts is crucial. Many methods have been developed to predict residual stress and deformation of LAM parts, including coupled thermal–mechanical model methods, multiscale modeling methods and modified intrinsic strain methods, reduced-order models and machine learning, etc.

Coupled thermal–mechanical model

In a coupled thermal–mechanical model for LAM, two physical fields of stress and temperature interact. That is, while the temperature change affects the stress deformation, the stress deformation also affects the temperature. However, the overall coupled thermal–mechanical characteristics of the LAM process are very complex, and the coupled thermal–mechanical analysis of multiple scans using a fine mesh model is often very time-consuming. Zhao et al. [60] established a coupled thermal–mechanical model to simulate the thermal history and residual stress during the DMLS process of Ti6Al4V parts. The evolution of residual stress was analyzed, and the influence of substrate preheating temperature on residual stress was studied. Yang et al. [61] studied the

microstructure, hardness, residual stress and deformation of large-scale SLM parts. A transient coupled thermal-metallurgical model was established to predict the microstructure and hardness of large-scale SLMed 4140 steel parts, and a coupled thermal–mechanical model was established to predict the residual stress and deformation of large-scale SLMed Inconel 718 parts. And the reliability of the prediction model was verified by experiments. Zhang et al. [62] established a one-way coupled thermal–mechanical model to simulate the DMLS process to predict the deformation and cracking of DMLS parts. Nazami et al. [63] established a three-dimensional transient coupled thermal–mechanical model to predict the residual stress and deformation of AlSi10Mg parts during the DMLS process, and discussed the effect of laser spot overlap on the residual stress of the parts. Mukherjee et al. [64] combined a 3D transient heat transfer and fluid flow model with a coupled thermal–mechanical model to calculate the temperature field, residual stress and deformation of the LDM, and predicted the residual stress and deformation of Ti6Al4V and Inconel 718 parts fabricated under different process parameters.

Multiscale modeling methods

Although the macroscopic model of LAM part deformation has the advantage of a small amount of calculation, it is difficult to reflect the microscopic mechanism of part deformation. Due to the limitation of computer power and modeling workload, it is unrealistic to use microscopic models to simulate complex structural parts. Therefore, there is a need for a computational model that can simulate both local microscopic changes and macroscopic deformations of parts. Multiscale model can be used to study the properties of materials at different lengths and time scales, providing a bridge to connect models at different scales, allowing models applicable at different scales to communicate with each other to study different properties of materials. Li [65–67] et al. developed a multi-scale modeling method to rapidly predict the residual stress and deformation of SLM parts, by integrating micro-scale laser scanning model, meso-scale layer filling model and macro-scale part model to quickly predict part deformation. The deformation of part fabricated with different scanning strategy was measured and the model was experimentally validated. On the basis of this method, two multiscale methods based on temperature-thread and stress-thread were developed and compared, and it was found that the deformation predicted by the multiscale method based on temperature-thread is closer to the measured result. Subsequently, a multi-scale modeling method based on temperature-thread was used to predict the residual stress and deformation of double cantilever beam parts, and the maximum deformation error was 28%.

Modified intrinsic strain method

Intrinsic strain method is widely used in welding problems. The inherent strain is the source of residual stress and weld cracks. If the inherent strain is known, the residual stress and deformation can be calculated by thermal elastic–plastic finite element analysis. Since the thermal deformation of AM is similar in principle to that of welding, the inherent strain method has been applied to additive manufacturing field. However, if the traditional intrinsic strain theory is directly applied to AM, the residual stress and deformation of the part cannot be predicted accurately. Liang and Chen [68–71] from the Department of Mechanical Engineering and Materials Science of the University of Pittsburgh, conducted a lot of research on the deformation prediction of LAM based on the inherent strain method. Based on the traditional intrinsic strain method, the modified intrinsic strain theory was proposed, which was applied to DMLS thin-walled parts and double-cantilever beam parts, and the stress prediction and dimensional deformation prediction of large-scale parts were realized. Subsequently, the improved intrinsic strain method was extended to the deformation simulation of large-scale SLM part fabricated with thin-walled support structures, and combined with asymptotic homogenization method to obtain equivalent mechanical properties including anisotropic elastic modulus and intrinsic strain. Lyu et al. [72] modified the traditional intrinsic strain method, calculated the intrinsic strain by simulating the thermo-mechanical process at a small scale, and considered the physical state of the deposited material in the simulation, and then applied the extracted intrinsic strain to double- cantilever beams and gears to predict the residual stress and deformation of the SLM parts. Setien et al. [73] established a mathematical model based on the intrinsic strain method to predict the residual stress and deformation of SLM large-scale Ti6Al4V parts. The model was validated experimentally by fabricating double-cantilever parts with different scanning strategies and measuring their deformations.

Reduced-order model

The deformation simulation of LAM parts is generally described by differential equations, and the dimensions of the equations are usually relatively high, which brings great challenges to engineers. The reduced-order model is a low-dimensional approximate description of the multi-dimensional physical process that changes with time, which can reduce the calculation amount and save the calculation time. The reduced-order model possesses a faster calculation speed, especially in the case of more degrees of freedom, but less information is retained in the original system and the model accuracy will be lowered. Ha et al. [74] proposed

two-dimensional and three-dimensional finite element models considering solidification effects, in order to analyze the effect of temperature gradient and sequential solidification on residual stress in a single bead that was cooled rapidly during the LDM process. A reduced-order model was also proposed, which successfully predicted the residual stress during the deposition of a single bead during sequential solidification in LAM. Ghnatios et al. [75] proposed a coupled thermal–mechanical model and its associated reduced-order model to evaluate part deformation. This model was used to predict the maximum deflection of LAM formed stainless steel 316L cantilevered plate and the predicted simulated results were in excellent agreement with the experimental measurement value.

Machine learning

Machine Learning (ML) is a study of computer algorithms that can automatically improve data analysis models through huge data sets and continuous training. In ML, models are continuously trained to discover patterns and correlations from large amounts of data, and then make optimal decisions and predictions based on the results of data analysis. The prediction accuracy increases with the increase of data. Deep Learning (DL) is a method of ML and called "deep" because the technique uses multiple layers of neural networks and large amounts of complex, disparate data. Francis et al. [76] developed a DL model to predict distortion by considering the local heat transfer for pointwise distortion prediction. The model was used to predict the deformation of Ti6Al4V parts manufactured by LAM, and the results showed that the model could accurately predict the deformation of the parts. Zhu et al. [77] proposed a DL method based on convolutional neural network to predict the geometric deviation of SLM parts with different shapes and process parameters. A data augmentation technique was introduced to generate samples for network training with a small amount of data. This method could effectively predict the geometric deviation of cylindrical shape and square shape parts. Mehrpouya et al. [78] developed a ML prediction tool based on artificial neural network to predict the transformation temperature and sample width of NiTiHf alloys with different process parameters, in order to study the effect of different process parameters on the transformation temperature and size deviation of SLM formed parts. The results predicted by the model were in good agreement with experimental measurements.

In the residual stress and deformation prediction of LAM parts, in order to obtain satisfying prediction accuracy, the simulation method requires a huge amount of calculation, and the ML method requires a large amount of data for training, which greatly reduces the work efficiency. Multiscale modeling and reduced-order model can reduce the calculation amount of the prediction model, but the models also need to ensure sufficient prediction accuracy, so the effect of shortening the calculation time is not ideal in some cases. In recent years, some researchers have begun to use reduced-order models combined with ML to reduce computational costs [79, 80], and more research can be invested in this area.

Deformation compensation of LAM metal parts

The deformation of LAM parts has a great impact on the size and quality of the parts. In order to eliminate or mitigate this effect, efforts have been taken to compensate for the deformation of the parts. Based on the deformation prediction for LAM, the deformation of the part can be inversely compensated to the initial geometry of the manufactured part to eliminate or reduce the deformation of the part, as shown in Fig. 11.

Biegler et al. [81] compensated the deformation inversely to the initial geometry of part, and used a coupled thermal–mechanical model to simulate the shape of the LDM formed 316L thin-walled curved turbine blade after deformation compensation. Then experiments proved that this compensation method could also be applied to other large-scale parts. Babkin et al. [82] established a two-dimensional coupled thermal–mechanical model for predicting the deformation of LDM large-scale axisymmetric Ti6Al4V cylinder parts. The deformation predicted by the model was reversely compensated to the initial geometry of the part, and then the model was used again to predict the shape and size of

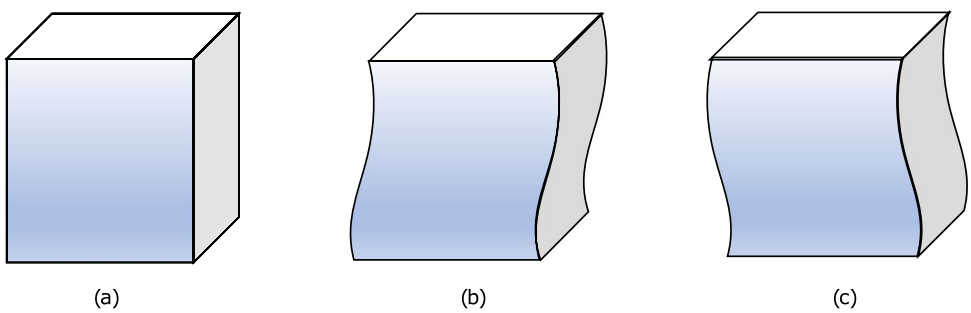

Fig. 11 Distortion inversion compensation concept (**a**) part to be formed; (**b**) part after deformation; (**c**) formed part after reverse compensation

the formed part after compensation. The simulation results were in good agreement with the experimental results. Zhang et al. [83] adopted a mathematical model based on intrinsic strain to predict the deformation of DMLS parts, and applied nonlinear least squares NURBS surfaces construction to compensate for the part geometry. The original and compensated geometries were imported into the model and the deformation results before and after compensation were compared. The flatness error and cylindricity error of the two test parts were measured respectively, and it was found that the cylindrical error and flatness error of the compensated parts were significantly reduced. Afazov et al. [84] developed a deformation compensation method based on 3D optical scanning data, conducted deformation prediction for SLM manufactured Inconel 718 turbine blades and impeller parts, and then compensated the original geometry. The experiments showed that the compensation reduced the deformation of blades and impellers from about 300 μm to about 65 μm. Subsequently, Afazov et al. [85] improved the mathematical model proposed by Afazov [84] to predict the deformation of the LDM manufactured Inconel 718 manifold structure. The experiments demonstrated that the improved method reduced the deformation of the manifold structure from around 400 μm to around 100 μm.

Conclusion and prospect

In this paper, the research status of residual stress and deformation for LAM parts is reviewed. The main factors affecting the deformation, the commonly used residual stress and deformation measure methods, and the deformation prediction and compensation methods of LAM parts are summarized. The following conclusions are drawn.

(1) Due to the multiple thermal cycles in the LAM process, the residual stress and deformation of the parts vary non-linearly with process parameters and other factors. When only single-scan is investigated, and the process parameters may tend to have different effects on residual stress and deformation of metal parts manufactured by LAM.
(2) In recent years, with the development of measuring method for residual stress and deformation of metal parts manufactured by LAM, in order to avoid damage to the test piece, non-destructive testing method has been paid more and more attention and used widely by researchers. Among them, the optical measurement method is used most widely due to its non-contact and other advantages.
(3) In terms of residual stress and deformation prediction of LAM metal parts, the calculation amount of simulation and the amount of data required by ML are relatively large. To significantly reduce computational costs and improve work efficiency, efforts can be taken to investigate methods that combine reduced-order models with ML.
(4) Through the pre-deformation analysis of the part, the deformation of the part is reversely compensated to the initial geometric position of the manufactured part, which can better reduce the final deformation of the part. The method can improve the dimensional accuracy of LAM, and has a good application prospect.

In the researches on residual stress and deformation of LAM parts, no breakthrough has been made in the full-field deformation detection during the manufacturing process of LAM parts. Prediction will be the main research direction in the next few years. In the existing literatures on the detection of deformation process of LAM, the widely used method is the digital image correlation method. Due to the principle of the digital image correlation method, the digital image correlation method before requires creating speckles on the surface of the manufactured part, and measuring the deformation of the part with the speckle pattern. The deformation of LAM parts at the beginning of manufacturing cannot be measured. In recent years, the research and application of binocular vision measurement method has gradually increased. This method has the advantages of high efficiency, simple structure, non-contact measurement, etc., and can be applied to deformation detection during the LAM process. However, the accuracy of binocular vision measurement is not high enough currently, which is a key problem that needs to be overcome in the future research.

Acknowledgements The work was supported by the National Key Research and Development Program of China (Grant No. 2021YFC2801904) and the Central Guidance on Local Science and Technology Development Fund of Liaoning Province (Grant No. 2022JH6/100100041).

Declarations

Conflict of interest/Competing interest The authors declare that they have no conflict of interest nor competing interest.

References

1. Nandy J, Sarangi H, Sahoo S (2019) A Review on Direct Metal Laser Sintering: Process Features and Microstructure Modeling. Lasers Manuf Mater Process 6:280–316. https://doi.org/10.1007/s40516-019-00094-y
2. Plotkowski A, Rios O, Sridharan N, Sims Z, Unocic K, Ott R, Dehoff R, Babu SS (2017) Evaluation of an Al-Ce alloy for laser additive manufacturing. Acta Mater 126:507–519. https://doi.org/10.1016/j.actamat.2016.12.065
3. Wen P, Voshage M, Jauer L, Chen Y, Qin Y, Poprawe R, Schleifenbaum JH (2018) Laser additive manufacturing of Zn metal parts for biodegradable applications: Processing, formation quality and

mechanical properties. Mater Des 155:36–45. https://doi.org/10.1016/j.matdes.2018.05.057
4. Yang Y, Lu C, Peng S, Shen L, Wang D, Qi F, Shuai C (2020) Laser additive manufacturing of Mg-based composite with improved degradation behaviour. Virtual Phys Prototyping 15:278–293. https://doi.org/10.1080/17452759.2020.1748381
5. Bremen S, Meiners W, Diatlov A (2012) Selective Laser Melting: a Manufacturing Technology for the Future. Laser Tech J 9:33–38. https://doi.org/10.1002/latj.201290018
6. Gibson I, Rosen D, Stucker B (2015) Directed energy deposition processes. In: Additive manufacturing technologies, 2nd edn. Springer, New York, pp 245–268. https://doi.org/10.1007/978-1-4939-2113-3_10
7. Safronov VA, Khmyrov RS, Kotoban DV, Gusarov AV (2017) Distortions and Residual Stresses at Layer-by-Layer Additive Manufacturing by Fusion. J Manuf Sci Eng 139:031017. https://doi.org/10.1115/1.4034714
8. Bambach M, Sizova I, Szyndler J, Bennett J, Hyatt G, Cao J, Papke T, Merklein M (2020) On the hot deformation behavior of Ti-6Al-4V made by additive manufacturing. J Mater Process Technol 288:116840. https://doi.org/10.1016/j.jmatprotec.2020.116840
9. Mercelis P, Kruth JP (2006) Residual stresses in selective laser sintering and selective laser melting. Rapid Prototyping Journal 12:254–265. https://doi.org/10.1108/13552540610707013
10. Van Zyl I, Yadroitsava I, Yadroitsev I (2015) Residual stresses in direct metal laser sintered parts. Interim Interdiscip J 14:110–123
11. Kayacan MY, Özsoy K, Duman B, Yilmaz N, Kayacan MC (2019) A study on elimination of failures resulting from layering and internal stresses in Powder Bed Fusion (PBF) additive manufacturing. Mater Manuf Processes 34:1467–1475. https://doi.org/10.1080/10426914.2019.1655151
12. Paul R, Anand S, Gerner F (2014) Effect of Thermal Deformation on Part Errors in Metal Powder Based Additive Manufacturing Processes. J Manuf Sci Eng 136:031009. https://doi.org/10.1115/1.4026524
13. Saphronov V, Khmyrov RS, Gusarov AV (2015) Experimental and theoretical study of residual deformations and stresses at additive manufacturing by fusion. ResearchGate. https://www.researchgate.net/publication/349339894. Accessed 16 Feb 2021
14. Mugwagwa L, Dimitrov D, Matope S, Muvunzi R (2016) Residual stresses and distortions in selective laser melting-a review. ResearchGate. https://www.researchgate.net/publication/318014975. Accessed 25 June 2019
15. Fang ZC, Wu ZL, Huang CG, Wu CW (2020) Review on residual stress in selective laser melting additive manufacturing of alloy parts. Opt Laser Technol 129:106283. https://doi.org/10.1016/j.optlastec.2020.106283
16. Ali H, Ghadbeigi H, Mumtaz K (2018) Processing Parameter Effects on Residual Stress and Mechanical Properties of Selective Laser Melted Ti6Al4V. J Mater Eng Perform 27:4059–4068. https://doi.org/10.1007/s11665-018-3477-5
17. Mugwagwa L, Dimitrov D, Matope S, Yadroitsev I (2018) Influence of process parameters on residual stress related distortions in selective laser melting. Procedia Manuf 21:92–99. https://doi.org/10.1016/j.promfg.2018.02.099
18. Jiang X, Ye Y, Zhu Y (2020) Effect of process parameters on residual stress in selective laser melting of AlSi10Mg. Mater Sci Techno 36:342–352. https://doi.org/10.1080/02670836.2019.1705560
19. Malý M, Höller C, Skalon M, Meier B, Koutný D, Pichler R, Sommitsch C, Paloušek D (2019) Effect of Process Parameters and High-Temperature Preheating on Residual Stress and Relative Density of Ti6Al4V Processed by Selective Laser Melting. Materials 12:930. https://doi.org/10.3390/ma12060930
20. Levkulich NC, Semiatin SL, Gockel JE, Middendorf JR, DeWald AT, Klingbeil NW (2019) The Effect of Process Parameters on Residual Stress Evolution and Distortion in the Laser Powder Bed Fusion of Ti-6Al-4V. Addit Manuf 28:475–484. https://doi.org/10.1016/j.addma.2019.05.015
21. Xiao Z, Chen C, Zhu H, Hu Z, Nagarajan B, Guo L, Zeng X (2020) Study of residual stress in selective laser melting of Ti6Al4V. Mater Des 193:108846. https://doi.org/10.1016/j.matdes.2020.108846
22. Cheng B, Shrestha S, Chou K (2016) Stress and deformation evaluations of scanning strategy effect in selective laser melting. Addit Manuf 12:240–251. https://doi.org/10.1016/j.addma.2016.05.007
23. Ali H, Ghadbeigi H, Mumtaz K (2018) Effect of scanning strategies on residual stress and mechanical properties of Selective Laser Melted Ti6Al4V. Mater Sci Eng 712:175–187. https://doi.org/10.1016/j.msea.2017.11.103
24. Song J, Wu WH, Zhang L, He BB, Lu L, Ni XQ, Long QL, Zhu GL (2018) Role of scanning strategy on residual stress distribution in Ti-6Al-4V alloy prepared by selective laser melting. Optik 170:342–352. https://doi.org/10.1016/j.ijleo.2018.05.128
25. Wang D, Wu SB, Yang YQ, Dou WH, Deng SS, Wang Z, Li S (2018) The Effect of a Scanning Strategy on the Residual Stress of 316L Steel Parts Fabricated by Selective Laser Melting (SLM). Materials 11:1821. https://doi.org/10.3390/ma11101821
26. Mugwagwa L, Dimitrov D, Matope S, Yadroitsev I (2019) Evaluation of the impact of scanning strategies on residual stresses in selective laser melting. Int J Adv Manuf Technol 102:2441–2450. https://doi.org/10.1007/s00170-019-03396-9
27. Guo J, Haiyang FU, Pan B, Kang R (2021) Recent Progress of Residual Stress Measurement Methods: A Review. Chin J Aeronaut 34:54–78. https://doi.org/10.1016/j.cja.2019.10.010
28. Heigel JC, Michaleris P, Reutzel EW (2015) Thermo-mechanical model development and validation of directed energy deposition additive manufacturing of Ti-6Al-4V. Addit Manuf 5:9–19. https://doi.org/10.1016/j.addma.2014.10.003
29. Prime MB, Dewald AT (2013) The contour method. In: Practical residual stress measurement methods, 1st edn. Wiley, New York, pp 109–138. https://doi.org/10.1002/9781118402832.ch5
30. Vrancken B, Cain V, Knutsen R, Humbeeck JV (2014) Residual stress via the contour method in compact tension specimens produced via selective laser melting. Scr Mater 87:29–32. https://doi.org/10.1016/j.scriptamat.2014.05.016
31. Ahmad B, Veen SOD, Fitzpatrick ME, Guo H (2018) Residual stress evaluation in selective-laser-melting additively manufactured titanium (Ti-6Al-4V) and inconel 718 using the contour method and numerical simulation. Addit Manuf 22:571–582. https://doi.org/10.1016/j.addma.2018.06.002
32. Prevéy PS (1986) X-ray diffraction residual stress techniques. Metals Handbook, American Society for Metals, OH, pp 380-392
33. Lin J, Ma N, Lei Y, Murakawa H (2017) Measurement of residual stress in arc welded lap joints by cosα X-ray diffraction method. J Mater Process Technol 243:387–394. https://doi.org/10.1016/j.jmatprotec.2016.12.021
34. Prevéy PS (1996) Current applications of X-ray diffraction residual stress measurement. Developments in materials characterization technologies, OH, pp 103–110
35. Fitzpatrick ME, Fry AT, Holdway P, Kandil FA, Shackleton J, Suominen L (2005) Determination of residual stresses by X-ray diffraction - Issue 2. National Physical Laboratory. http://eprintspublications.npl.co.uk/id/eprint/2391. Accessed 02 Feb 2018
36. Simson T, Emmela A, Dwars A, Böhm J (2017) Residual stress measurements on AISI 316L samples manufactured by selective laser melting. Addit Manuf 17:183–189. https://doi.org/10.1016/j.addma.2017.07.007

37. Kumaran M, Lkumar VS, Panicker CTJ, Shishir R (2021) Investigating the residual stress in additive manufacturing of combined process in powder bed fusion and directed energy deposition. Mater Today Proc 47:4387-4390.https://doi.org/10.1016/j.matpr.2021.05.200
38. Park MJ, Yang HN, Jang DY, Kim JS, Jin TE (2004) Residual stress measurement on welded specimen by neutron diffraction. J Mater Process Techno 155–156:1171–1177. https://doi.org/10.1016/j.jmatprotec.2004.04.393
39. Rangaswamy P, Griffith ML, Prime MB, Holden TM, Rogge RB, Edwards JM, Sebring RJ (2005) Residual stresses in LENS components using neutron diffraction and contour method. Mater Sci Eng A 399:72–83. https://doi.org/10.1016/j.msea.2005.02.019
40. Paradowska A, Price JWH, Ibrahim R, Finlayson T (2005) A neutron diffraction study of residual stress due to welding. J Mater Process Technol 164–165:1099–1105. https://doi.org/10.1016/j.jmatprotec.2005.02.092
41. Wang Z, Denlinger E, Michaleris P, Stoica AD, Ma D, Beese AM (2017) Residual stress mapping in Inconel 625 fabricated through additive manufacturing: Method for neutron diffraction measurements to validate thermomechanical model predictions. Mater Des 113:169–177. https://doi.org/10.1016/j.matdes.2016.10.003
42. Wang ZQ, Stoica AD, Ma D, Beese AM (2017) Stress relaxation behavior and mechanisms in Ti-6Al-4V determined via in situ neutron diffraction: Application to additive manufacturing. Mater Sci Eng A 707:585–592. https://doi.org/10.1016/j.msea.2017.09.071
43. Kemerling B, Lippold JC, Fancher CM, Bunn J (2018) Residual stress evaluation of components produced via direct metal laser sintering. Weld World 62:663–674. https://doi.org/10.1007/s40194-018-0572-z
44. Wozniak A, Dobosz M (2005) Factors influencing probing accuracy of a coordinate measuring machine. IEEE Trans Instrum Meas 54:2540–2548. https://doi.org/10.1109/TIM.2005.858541
45. Dunbar AJ, Denlinger ER, Gouge MF, Michaleris P (2016) Experimental Validation of Finite Element Modeling for Laser Powder Bed Fusion Deformation. Addit Manuf 12:108–120. https://doi.org/10.1016/j.addma.2016.08.003
46. Ning JQ, Praniewicz M, Wang WJ, Dobbs JR, Liang SY (2020) Analytical modeling of part distortion in metal additive manufacturing. Int J Adv Manuf Technol 107:49–57. https://doi.org/10.1007/s00170-020-05065-8
47. Sun WJ, Brown S, Leach R (2012) An overview of industrial X-ray computed tomography. National Physical Laboratory. http://eprintspublications.npl.co.uk/id/eprint/5385. Accessed 02 Feb 2018
48. Thompson A, Maskery I, Leach RK (2016) X-ray computed tomography for additive manufacturing: a review. Meas Sci Technol 27:072001
49. Samei J, Amirmaleki M, Ventura AP, Pawlikowski GT, Bayes M, Misiolek WZ, Wilkinson DS (2020) In-situ X-ray Tomography Analysis of the Evolution of Pores during Deformation of a Cu-Sn Alloy Fabricated by Selective Laser Melting. Addit Manuf 34:101196. https://doi.org/10.1016/j.addma.2020.101196
50. Choo H, White LP, Xiao XH, Sluss CC, Morin D, Garlea C (2021) Deformation and fracture behavior of a laser powder bed fusion processed stainless steel: In situ synchrotron x-ray computed microtomography study. Addit Manuf 40:101914. https://doi.org/10.1016/j.addma.2021.101914
51. Song HX, Wang XD, Ma LQ, Cai MZ, Cao TZ (2006) Design and performance analysis of laser displacement sensor based on position sensitive detector (PSD). J Phys Conf Ser 48:040. https://doi.org/10.1088/1742-6596/48/1/040
52. Sun JH, Zhang J, Liu Z, Zhang GJ (2013) A vision measurement model of laser displacement sensor and its calibration method. Opt Lasers Eng 51:1344–1352. https://doi.org/10.1016/j.optlaseng.2013.05.009
53. Denlinger ER, Heigel JC, Michaleris P, Palmer TA (2015) Effect of inter-layer dwell time on distortion and residual stress in additive manufacturing of titanium and nickel alloys. J Mater Process Techno 215:123–131. https://doi.org/10.1016/j.jmatprotec.2014.07.030
54. Corbin DJ, Nassarc AR, Reutzelc EW, Kistlerb NA, Beeseb AM, Michalerisa P (2016) Impact of directed energy deposition parameters on mechanical distortion of laser deposited Ti-6Al-4V. In: 2016 International Solid Freeform Fabrication Symposium. Austin, Texas, pp 670–679
55. McCormick N, Lord J (2010) Digital image correlation. Mater Today 13:52–54. https://doi.org/10.1016/S1369-7021(10)70235-2
56. Pan B (2011) Recent Progress in Digital Image Correlation. Exp Mech 51:1223–1235. https://doi.org/10.1007/s11340-010-9418-3
57. Biegler M, Marko A, Graf B, Rethmeier M (2018) Finite element analysis of in-situ distortion and bulging for an arbitrarily curved additive manufacturing directed energy deposition geometry. Addit Manuf 24:264–272. https://doi.org/10.1016/j.addma.2018.10.006
58. Balit Y, Charkaluk E, Constantinescu A (2020) Digital image correlation for microstructural analysis of deformation pattern in additively manufactured 316L thin walls. Addit Manuf 31:100862. https://doi.org/10.1016/j.addma.2019.100862
59. Wu MW, Chen JK, Chiang PH, Chang PM, Tsai MK (2020) Compression Property, Deformation Behavior, and Fracture Mechanism of Additive-Manufactured Ti-6Al-4V Cellular Solid with a New Cuboctahedron Structure. Metall Mater Trans A 51:6517–6527. https://doi.org/10.1007/s11661-020-06013-7
60. Zhao X, Iyer A, Promoppatum P, Yao S (2017) Numerical modeling of the thermal behavior and residual stress in the direct metal laser sintering process of titanium alloy products. Addit Manuf 14:126–136. https://doi.org/10.1016/j.addma.2016.10.005
61. Yang YP, Jamshidinia M, Boulware P, Kelly SM (2017) Prediction of microstructure, residual stress, and deformation in laser powder bed fusion process. Comput Mech 61:599–615. https://doi.org/10.1007/s00466-017-1528-7
62. Zhang Y, Zhang J (2017) Finite Element Simulation and Experimental Validation of Distortion and Cracking Failure Phenomena in Direct Metal Laser Sintering Fabricated Component. Addit Manuf 16:49–57. https://doi.org/10.1016/j.addma.2017.05.002
63. Nazami GR, Pandab BK, Sahoo S (2021) Finite element simulation of residual stress in direct metal laser sintering of AlSi10Mg built part: Effect of laser spot overlapping. Mater Today Proc 41:445–450. https://doi.org/10.1016/j.matpr.2020.09.844
64. Mukherjee T, Zhang W, Debroy T (2017) An improved prediction of residual stresses and distortion in additive manufacturing. Comput Mater Sci 126:360–372. https://doi.org/10.1016/j.commatsci.2016.10.003
65. Li C, Fu CH, Guo YB, Fang FZ (2016) A Multiscale Modeling Approach for Fast Prediction of Part Distortion in Selective Laser Melting. J Mater Process Technol 229:703–712. https://doi.org/10.1016/j.jmatprotec.2015.10.022
66. Li C, Liu JF, Guo YB (2016) Prediction of Residual Stress and Part Distortion in Selective Laser Melting. Procedia Cirp 45:171–174. https://doi.org/10.1016/j.procir.2016.02.058
67. Li C, Liu JF, Fang XY, Guo YB (2017) Efficient predictive model of part distortion and residual stress in selective laser melting. Addit Manuf 17:157–168. https://doi.org/10.1016/j.addma.2017.08.014
68. Liang X, Chen Q, Cheng L, Yang QC, To A (2017) A modified inherent strain method for fast prediction of residual deformation in additive manufacturing of metal parts. In: 2017 Solid Freeform Fabrication Symposium Proceedings. Austin, Texas, pp 2539–2545. https://doi.org/10.26153/tsw/16972

69. Chen Q, Liang X, Haydukeb D, Liua J, Cheng L, Oskinaet J, Whitmoreb R, To A (2019) An inherent strain based multiscale modeling framework for simulating part-scale residual deformation for direct metal laser sintering. Addit Manuf 28:406–418. https://doi.org/10.1016/j.addma.2019.05.021
70. Liang X, Chen Q, Cheng L, Hayduke D, To AC (2019) Modified inherent strain method for efficient prediction of residual deformation in direct metal laser sintered components. Comput Mech 64:1719–1733. https://doi.org/10.1007/s00466-019-01748-6
71. Lianga X, Donga W, Hinnebuscha S, Chen Q, Tran HT, Lemon J, Cheng L, Zhou Z, Hayduke D, To AC (2020) Inherent strain homogenization for fast residual deformation simulation of thin-walled lattice support structures built by laser powder bed fusion additive manufacturing. Addit Manuf 32:101091. https://doi.org/10.1016/j.addma.2020.101091
72. Lyu DD, Hu W, Pan XF, Wu CT (2020) Numerical Prediction of Residual Deformation and Failure for Powder Bed Fusion Additive Manufacturing of Metal Parts. J Mech 36:1–14. https://doi.org/10.1017/jmech.2020.30
73. Setien I, Chiumenti M, van der Veen S, Sebastian MS, Garciandía F, Echeverría A (2019) Empirical methodology to determine inherent strains in additive manufacturing. Comput Math Appl 78:2282–2295. https://doi.org/10.1016/j.camwa.2018.05.015
74. Ha K, Kim T, Baek GY, Jeon JB, Shim DS, Moon YH, Lee W (2020) Numerical study of the effect of progressive solidification on residual stress in single-bead-on-plate additive manufacturing. Addit Manuf 34:101245. https://doi.org/10.1016/j.addma.2020.101245
75. Ghnatios C, Rai KE, Hascoet N, Pires PA, Duval JL, Lambarri J, Hascoet JY, Chinesta F (2021) Reduced order modeling of selective laser melting: from calibration to parametric part distortion. Int J Mater Form 14:973–986. https://doi.org/10.1007/s12289-021-01613-z
76. Francis J, Bian L (2019) Deep learning for distortion prediction in laser-based additive manufacturing using big data. Manuf Lett 20:10–14. https://doi.org/10.1016/j.mfglet.2019.02.001
77. Zhu Z, Ferreira K, Anwer N, Mathieu L, Guo K, Qiao L (2020) Convolutional Neural Network for geometric deviation prediction in Additive Manufacturing. Procedia Cirp 91:534–539. https://doi.org/10.1016/j.procir.2020.03.108
78. Mehrpouya M, Gisario A, Nematollahi M, Rahimzadeh A, Baghbaderani KS, Elahinia M (2021) The prediction model for additively manufacturing of NiTiHf high-temperature shape memory alloy. Mater Today Commun 26:102022. https://doi.org/10.1016/j.mtcomm.2021.102022
79. Kallioras NA, Nordas AN, Lagaros ND (2021) Deep Learning-Based Accuracy Upgrade of Reduced Order Models in Topology Optimization. Appl Sci 11:12005. https://doi.org/10.3390/app112412005
80. Lu Y, Li H, Saha S, Mojumder S, Al Amin A, Suarez D, Liu Y, Qian D, Kam Liu W (2021) Reduced Order Machine Learning Finite Element Methods: Concept, Implementation, and Future Applications. Comput Model Eng Sci 129:1351–1371. https://doi.org/10.32604/cmes.2021.017719
81. Biegler M, Elsner BAM, Graf B, Rethmeier M (2020) Geometric distortion-compensation via transient numerical simulation for directed energy deposition additive manufacturing. Sci Technol Weld Joining 25:468–475. https://doi.org/10.1080/13621718.2020.1743927
82. Babkin K, Zemlyakovab E, Ivanov S, Vildanov A, Topalova I, Turichin G (2020) Distortion prediction and compensation in direct laser deposition of large axisymmetric Ti-6Al-4V part. Procedia CIRP 94:357–361. https://doi.org/10.1016/j.procir.2020.09.145
83. Zhang B, Li L, Anand S (2020) Distortion Prediction and NURBS Based Geometry Compensation for Reducing Part Errors in Additive Manufacturing. Procedia Manuf 48:706–717. https://doi.org/10.1016/j.promfg.2020.05.103
84. Afazov S, Okioga A, Holloway A, Denmark W, Triantaphyllou A, Smith S (2017) A methodology for precision additive manufacturing through compensation. Precis Eng 50:269–274
85. Afazov S, Semerdzhieva E, Scrimieri D, Serjouei A, Derguti F (2021) An improved distortion compensation approach for additive manufacturing using optically scanned data. Virtual Phys Prototyping 16:1–13. https://doi.org/10.1080/17452759.2021.1881702

Publisher's note Springer Nature remains neutral with regard to jurisdictional claims in published maps and institutional affiliations.

Springer Nature or its licensor (e.g. a society or other partner) holds exclusive rights to this article under a publishing agreement with the author(s) or other rightsholder(s); author self-archiving of the accepted manuscript version of this article is solely governed by the terms of such publishing agreement and applicable law.